

QD laser on InP substrate for 1.55 μm emission and beyond

N. Bertru^a, C. Paranthoen^a, O. Dehaese^a, H. Folliot^a, A. Le Corre^a, R. Piron^a, F. Grillot^a,
W. Lu^a, J. Even^a, G. Elias^a, C. Levallois^a, S. Loualiche^a, M. Bozkurt^b, J. Ulloa^b, P.
Koenraad^b, A. Ponchet^c

^a FOTON, INSA, Université Européenne de Bretagne Avenue des buttes de Coesmes F-35043, France.

^b eiTT/COBRA Inter-University Research Institute, Eindhoven University of Technology, P.O. Box 513, NL-5600MB Eindhoven, The Netherlands.

^c CEMES-Toulouse, 29, rue Jeanne Marvig, BP 9434731055 Toulouse Cedex 4 France

ABSTRACT

InAs nanostructures formed on InP substrates allow the realization of devices working in telecommunication wavelength range between 1.4 and 1.65 μm . However due to the low lattice mismatch existing between InAs and InP, the self assembling process in InP is more complex than on GaAs substrates. First high density quantum wires obtained on InP(001) have been integrated in laser. Lasers emitting at room temperature have been achieved. For an infinite length cavity, a threshold current density per QD plane as low as 45 A/cm² is deduced. This result compares favourably with those obtained on quantum wells lasers. However, the stability of the threshold current with temperature, predicted for quantum dots laser is not observed. Thus, growth on non standard substrates such as miscut substrates or high index substrates have been investigated in order to achieve QDs on InP. On (113) B substrates, quantum dots in high density and with size comparable with those achieved on GaAs(001) have been obtained. Lasers with record threshold current have been obtained. However the modulation properties of the laser are not as good as predicted for ideal quantum dots lasers. Finally we present the attempts to extend the QD emission wavelength in the 2-3 μm region.

Keywords : QD laser, Molecular beam epitaxy, InAs/InP nanostructure

1. INTRODUCTION

Semiconductor research and device development have seen a progressive reduction in dimensionality from bulk through quantum wells and quantum wires to quantum dots (QDs). QDs represent the ultimate limit in carrier confinement with discrete energy states.¹ Asada *et al*² predicted since 1986 that perfect QD ensembles can allow the achievement of lasers with improved performances. At the end of the 1990s it was realized that the Stranski-Krastanow (SK) growth mode occurring during the growth of lattice mismatched materials can be used to form high densities of homogenous QDs.³ The prototype system for SK QDs is InAs on GaAs where the lattice mismatch is 7.2 %. In this system various devices have been achieved and some of the predicted advantages for QD lasers such as lower threshold current density, improved thermal stability and the extension of the emission wavelength achievable on GaAs have been demonstrated.⁴ Moreover,

* nicolas.bertru @insa-rennes.fr

improvements have been also demonstrated in others devices useful for telecom network such as semiconductor optical amplifiers⁵ or mode lock lasers.⁶ Most of QD devices have been achieved on GaAs substrates with laser wavelengths ranging from 1 μm to 1.3 μm . Longer wavelength is theoretically reachable on GaAs by enlarging the InAs QD size. However due to the increasing built in strain, the maximum wavelength is about 1.4 μm before the material quality degrades.⁷ Using InP substrates the lattice mismatch with InAs can be reduced to about the half value existing with GaAs. This allows an extension of the emission wavelength beyond 1.55 μm and the realization of devices for long haul optical network. However due to the lower lattice mismatch and the switch of group V elements at the interfaces, the formation of nanostructures (NS) on InP is much more complex than on GaAs. For example the deposit of few monolayer of InAs on InP (001) leads to the formation of a high density of wires/dashes extended in the [1-10] lattice direction or of a low density of large (> 50 nm) dots depending on the growth conditions. Due to these elaboration issues, most of devices operating on InP (100) substrates is based on quantum wire/dash nanostructures. Devices based on quantum wires have demonstrated the interest of the InAs nanostructures for devices working at 1.55 μm . For example ultra-wide band SOA with high dynamical properties has been reported⁸ or mode lock lasers required for stable clock operation has been demonstrated.⁹

Numbers of approaches have been proposed to reduce the dash like character of the nanostructures formed on InP. One way, first proposed by CHTM New Mexico¹⁰ consists in the deposition on InP vicinal surfaces. Atomic steps modify the indium surface diffusion and favour the formation of isotropic QDs. Another approach is based on the growth on high index substrates such as (113)B. The high surface energy density of (113)B surface leads to a large increase of the QD density. QD laser with low threshold current density has been achieved on (113)B substrates. A last solution relies on Sb incorporation within InAs layer which results in InAsSb QDs. The incorporation of Sb permits to increase the lattice mismatch from 3.2 % (InAs) to 10% (InSb) and thus should favours the formation of high quality QDs. This method first investigated by Fujitsu lab allows moreover an extend of the emission wavelength of quantum dots grown on InP substrates in the mid infrared windows existing between 2 and 2.7 μm .

The paper is organized as follows. Section 2 briefly describes quantum wires/dash lasers elaborated on nominal InP (001) substrates. Section 3 discusses the different approach to achieve high quality QDs on InP substrates. The performances of devices elaborated using these approaches are compared. The studies on the incorporation of Sb within InAs QDs are reviewed in section 4. In section 5, conclusion is drawn

2. NS FORMATION AND LASER ON InP (001).

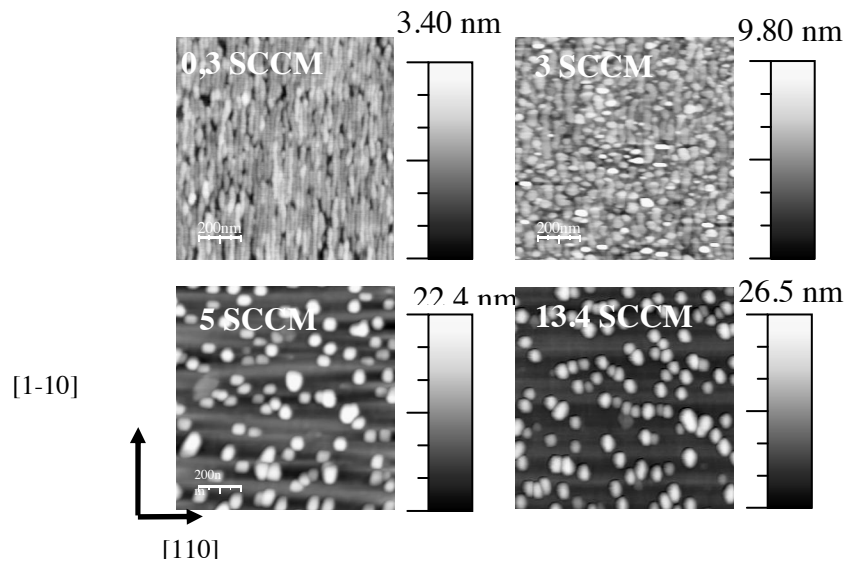


Figure 1. $1 \times 1 \mu\text{m}^2$ Atomic Force Microscopy (AFM) images from InAs nanostructures grown on GaInAsP alloy layers with various arsenine flow. The substrate temperature was set at 480°C and the amount of InAs deposited at 3.2 monolayer. The Z scale have been optimized for each image

First in order to present the difficulties related to the shape control of InAs/InP nanostructures, we reported in fig 1 Atomic Force Microscopy (AFM) images of InAs nanostructures formed on GaInAsP alloy (lattice matched to InP) layers with various As flux.¹¹ At low arsenic flux (0.3 sccm), high densities of NS elongated along [-110] directions are observed. Lateral dimensions are 25-30 nm along [110] direction and 200 to 400 nm along the other direction. The height in the growth direction is around 2-3 nm. Similar NS are obtained for deposit on different buffer material (i.e InGaAs, AlGaInAs or GaInAsP) and various growth techniques (Molecular beam epitaxy, Gas source MBE, or Chemical beam epitaxy). These elongated NS are named quantum Wires or Dashes. At higher arsenic flux (>5 SSCM) round shaped NS are observed. Their average lateral size is 64 nm and average height is 11 nm. The density achieved is around $1.2 \times 10^{10} \text{ cm}^{-2}$. In comparison with QDs formed on GaAs, the round shaped NS on InP are in low density and present large dimensions (Typical value on GaAs (001): density $>5 \times 10^{10} \text{ cm}^{-2}$ and diameter $\approx 25 \text{ nm}$). The densities of QDs reached are however low and their sizes are relatively large. Therefore only a reduced modal gain can be achieved which lead to the realization of reduced performance QD lasers.

Despite extensive studies reported on the formation of NS on InP, the trends which favour either quantum wires or quantum dots are not completely established.¹² It is mainly due to the As/P exchange existing at the InAs/InP interfaces and to a strong effect of buffer morphology on the NS shape. However it appears that large InAs deposits, long growth interrupts under arsenic flux and high arsenic fluxes during deposition favour the formation of isotropic shaped quantum dots.¹³ Different explanations for the elongated NS formation on InP substrates are given in literature. All explanations are based on the enhancement of the surface effects due to the low lattice mismatch existing between InAs and InP and on the large anisotropy of the (2x4) reconstructed InAs surfaces with dimer rows along the [-110] directions.¹⁴ However the detailed mechanism is still debated. As kinetic argument, the anisotropic ad-atoms diffusion on (2x4) reconstructed surfaces is suggested to favours the formation of elongated nanostructures. Thermodynamically, the anisotropy is interpreted in terms of different energies for formation of steps into the [-110] directions (A steps) and the [110] directions (B steps).¹⁵

Due to the low density of QDs achieved on nominal InP (100) surface, most of practical devices already reported are based on quantum wire/dash structures. On fig 2 we reported AFM image recorded on optimized quantum wires. From AFM image analysis, a mean height width and length of 2.2, 20 and 300 nm respectively are deduced. The typical areal density is $2 \times 10^{10} \text{ cm}^{-2}$. Five layers of Qwires were stacked in laser structures. The stripes of lasers were patterned along [110] direction which is perpendicular to the elongation of the Wires. This direction is chosen to obtain higher modal gain. Room temperature laser emission is observed at $1.58 \mu\text{m}$. The threshold current density versus reciprocal cavity length is reported figure 2. A current density for infinite length of 225 A/cm^2 is derived. It corresponds to a Jth of 45 A/cm^2 per Qwire layer. The characteristic temperature around room temperature was measured at 52 K. This value is comparable with value reported for QW laser. Note that an insensibility of Jth is predicted for ideal quantum dots. This discrepancy has been related to carrier leakage from the wires into the barrier region.

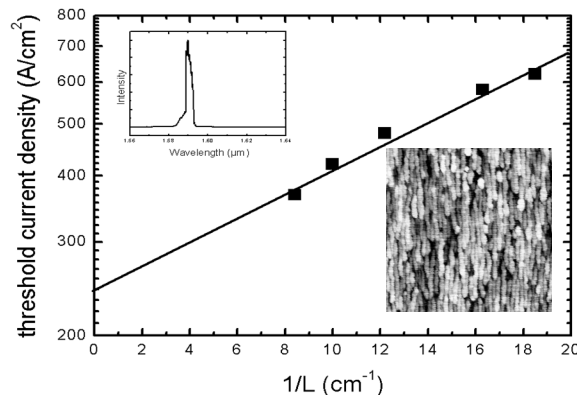


Figure 2. Threshold current density against reciprocal length taken at room temperature for a quantum wire laser
Inset: Lasing spectra for cavity length of 1.2 nm and AFM image taken on the first quantum wire plane

Considerable works have been performed by others groups on quantum wire/dash devices with different barriers materials (AlGaInAs) or structures (Dash in the Well). Reviews have been recently published.^{16,17} Briefly, threshold current values reported are comparable. The careful analysis of laser performances have shown that the characteristic temperatures (≈ 60 K) for devices with undoped active zones are not improved at room temperature for Qdash laser in comparison with QW ones. A Henry factor close to 0.5 has been measured below threshold. But in operating conditions (several time above threshold), Henry factor from four to six have been reported. More promising for telecom applications is the achievement of mode locked lasers with repetition rates greater than 300 GHz with low jitter down to 400 fs.¹⁸

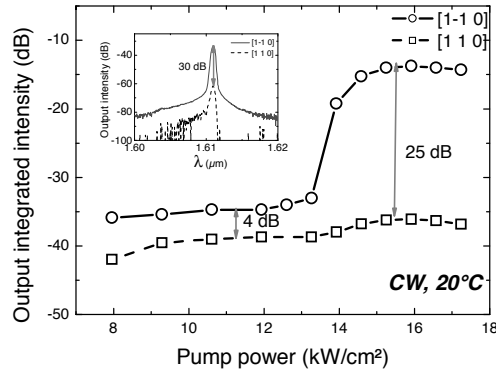


Figure. 3 Polarization resolved light output characteristics of a Qwire VCSEL versus the input optical power density Open circles (open squares) corresponds to the output intensity along the [110] direction ([110] respectively) Insets are spectra taken at 16 KW cm² pump power

Quantum wires have been integrated for the realization of a polarization controlled Vertical Cavity Surface Emitting Laser (VCSELS).¹⁹ On fig.3 is reported the integrated light output from a quantum wires VCSEL as a function of the optical excitation. Light output has been measured for light polarization along [110] and [1-10]. Below threshold (13 KW/cm²) the spontaneous emission shows a reduced polarization ratio of 4 dB. Above threshold the polarization is clamped along [1-10] direction with a polarization ratio higher than 25 dB. Thus the use of quantum wires structures allows to achieve polarization-controlled VCSEL emitting around 1.55 μm .

3. USE OF MISCUT SUBSTRATES OR HIGH INDEX SURFACES FOR QUANTUM DOTS ELABORATION ON INP

As stated in the previous section, the device performances are strongly dependant on how the carriers are confined. Therefore it is essential to control accurately the InAs/InP NS shape. Different approaches have been proposed to achieve small round shaped InAs QDs in high density on InP substrates.

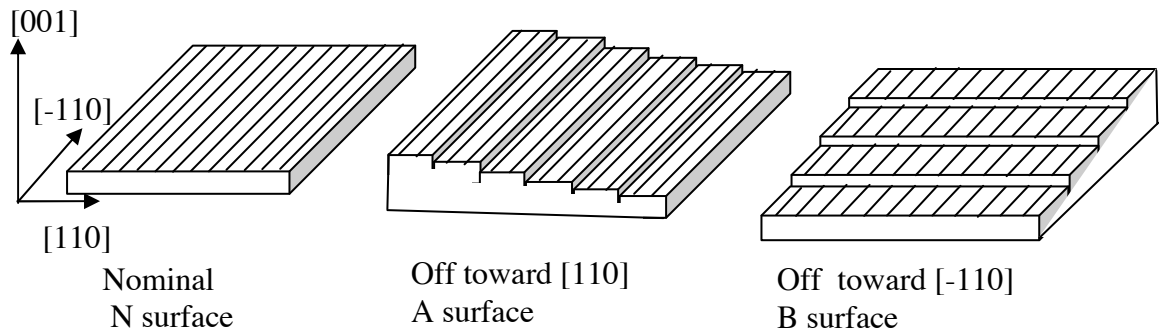


Figure 4. Surfaces of InP(001) substrates with different off-cut. Black lines along [-110] symbolize the dimer rows of the 2x4 reconstruction

The first approach in reducing the elongation of the quantum wires/dashes consists in the formation of NS on misoriented substrates.²⁰ Offcut substrates from InP (001) are commercially available towards [110] (A surfaces) and [-110] (B surfaces). The monolayer steps run parallel (A step) or perpendicular (B steps) to InAs nanowires (See figure 4).

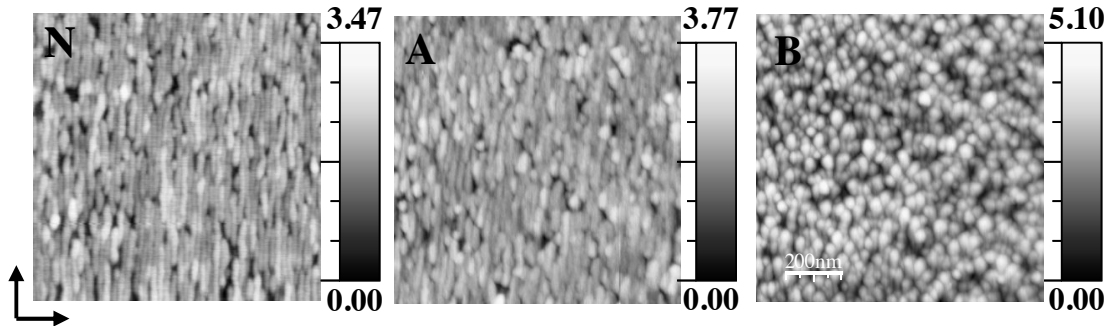


Figure 5. $1 \times 1 \mu\text{m}^2$ AFM Images from InAs nanostructures deposited on nominal, A and B surfaces (2° miscut) with a low arsenic flux (0.3 sccm). The Z scale was adjusted for each image.

On figure 5 are reported AFM images recorded after the deposition of 3 ML InAs on off-cut and nominal surfaces. On nominal and A surfaces, nanowires are obtained. The elongation is larger on exact substrates. On B surfaces, highly isotropic dots in high density ($7.10^{10} \text{ cm}^{-2}$) are achieved. The measured height and diameter are 2 nm and 30 nm respectively. Therefore dot formation is favoured when step edges run perpendicular to the direction of the dashes, but no change occurs when the step edges are parallel to the step structures. Similar results have been obtained by various groups.²¹ However, the effect of growth conditions on the NS shape is still discussed. For example, Bierwagen *et al*²² show that the nanostructure morphology is mainly dependent of miscut orientation and is independent of growth conditions. In marked contrast we observed that the As flux during deposition governs the NS shape. In our experiments, for growths performed under high As flux, the effect of the substrate misorientation is lost and low density of round shaped QDs are observed on any surface orientation.

Miscut substrates represent an effective way to achieve round shaped QDs on InP substrates. After optimization of the growth conditions, a QD density about $9.10^{10} \text{ cm}^{-2}$ and a PL emission around $1.55 \mu\text{m}$ have been achieved.²³ Laser structure emission at room temperature with a threshold current density of 1.06 kA/cm^2 for 1mm long cavity length has been reached. This result is comparable with results obtained on QDash structures (Figure 6.).

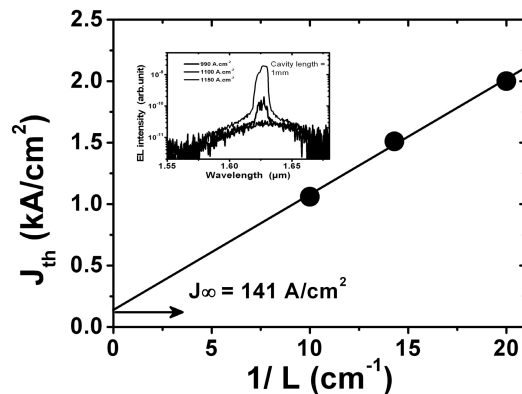


Figure 6. Threshold current density against reciprocal length taken at room temperature for a quantum dot laser achieved on B substrate. Inset: Lasing spectra for cavity length of 1 nm

A more radical method to achieve high quality QDs on InP substrates, consists in growing nanostructures on high index surfaces.²⁴ On figure 7 are reported AFM images after the deposition of 2.1 ML d'InAs on InP(100) and (113) B surfaces during the same growth run.

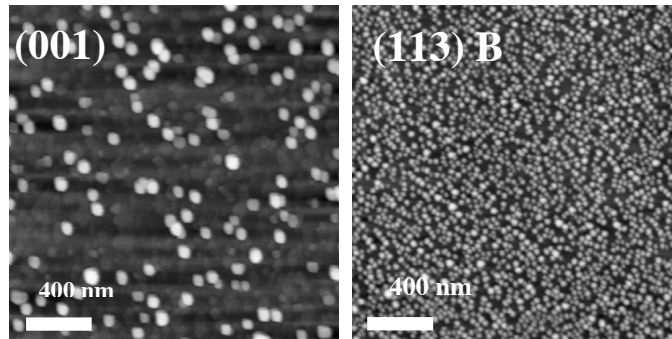


Figure 7. $2 \times 2 \mu\text{m}^2$ AFM image of islands formed after the deposition of 2.1 ML InAs on (001) and on (113)B substrates during the same growth run.

Low density ($< 5 \cdot 10^9 \text{ cm}^{-2}$) of large islands (diameter 70 nm) are observed on (001) surface. On the other hand on (113)B surface, higher density ($5 \cdot 10^{10} \text{ cm}^{-2}$) of smaller QDs (diameter 35 nm) is achieved. Therefore, under the same growth conditions the deposition on (113)B leads to the formation of an order of magnitude higher QD density. The QD diameters are the half than those obtained on (001). However QDs are still roughly twice larger than those of QD elaborated on GaAs substrates. Further growth condition optimisations have shown that the III/V pressure ratio is a key parameter to control the QD size on (311)B substrates. When decreasing the arsenic pressure, the QD mean height and radius are reduced to 4.8 and 12.0 nm respectively. The density reaches $1.6 \cdot 10^{11} \text{ cm}^{-2}$. These characteristics compare favourably with those of QDs achieved on GaAs substrates in standard conditions. The formation of high QD densities on (113)B surfaces has been related to the high surface energy density of high index surfaces. Indeed these surfaces are less stable than the (001) ones and therefore QDs nucleation is favoured. Such a surface effect compensates the low lattice mismatch between InAs and InP and leads to similar formation process of QDs on (113)B InP than to those observed on (001) GaAs.²⁵

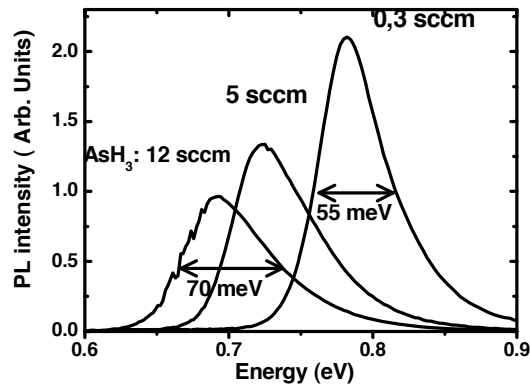


Figure 8. Room temperature PL spectra of InAs/InGaAsP QD samples grown with different AsH₃ flow rates

The RT PL spectra recorded on samples grown with various As pressure are shown on figure 8.²⁶ With the arsenic pressure decreasing, a shift to higher energy is observed. This trend is related to the smaller size of InAs QDs formed at low arsenic pressure. The FWHM of the PL peaks change from 70 meV to 55 meV. Despite the large improvement observed for low arsenic flux, the FWHM value of PL peaks for InAs/InP QDs is still considerably larger than for InAs/GaAs QDs on which a PL peak FWHM of 21 meV has been

reported.²⁷ Further improvements in size dispersion and geometry control were achieved by a discontinuous capping process named double cap during which the capping is performed in two sequences.²⁸

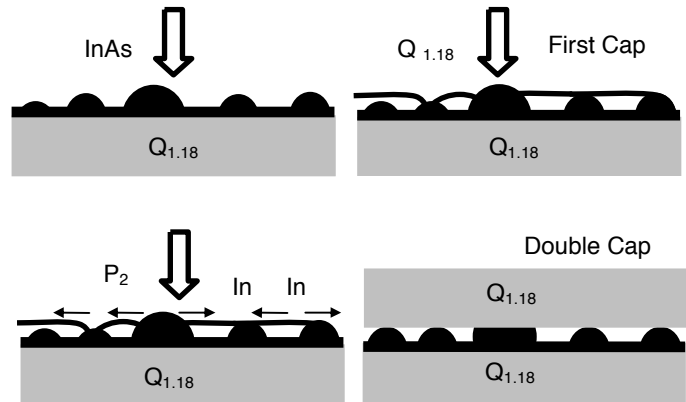


Figure 9. Schematic description of the growth steps during the double cap procedure.

A schematic description of the Double Cap (DC) process is reported on Fig 9. After the formation of QDs, a lattice matched capping layer is deposited. The thickness of this first cap layer is chosen to be thinner than the height of the larger dots. Due to high strain at the QD apex, this first cap layer (FCL) takes place between the dots. Then, a growth interruption under group V elements is performed, during which the uncovered part of the dots disappears due to As/P exchange, leading, in principle, to an uniform QD height equal to the thickness of the first thin capping layer.

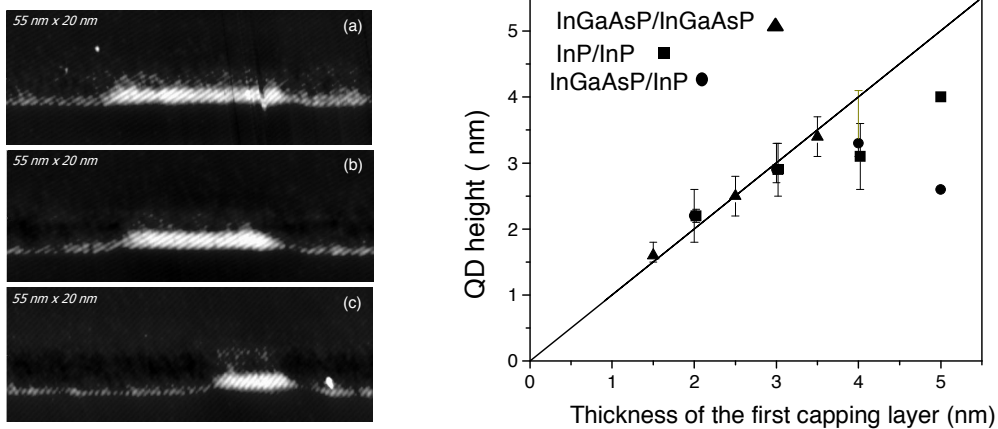


Figure 10. Left: Cross sectional STM images of the three QDs layer corresponding to first cap layer of 2 nm, 4 nm and 5 nm. The bright spots correspond to As atoms in the InP matrix. Right: Average QD height in each layer as a function of the nominal thickness of FCL for different nature of cap layers or (and) barriers. The solid curve represents the predicted QD height considering that the dot height corresponds exactly to the thickness of FCL.

Figure 10 shows cross sectional scanning tunnelling microscopy (X-STM) from a sample where three dot layers have been grown and DC cap method has been applied with various thickness of the FCL.²⁹ The buffer and capping layers consist in GaInAsP alloys usually used in 1.55 μm laser active zone. On fig 10, we observe that the height of the QDs increases when the thickness of FCL increases. The height of the QDs in each layer fits very well with the nominal thickness of FCL. After analyzing number of dots, the measured average height in layer a, is 1.6 nm, in layer b, 2.5 nm, and in layer c, 3.4 nm for FCL thickness of 1.5, 2.5 and

3.5 nm respectively. This indicates that the double capping procedure is controlling the QD height with high accuracy.

In order to achieve high gain and thus low threshold current density laser, it is essential to be able to control the stacking of QD layers. When DC technique is not used together with a thin spacer (10 nm) is deposited, a large shift to the low energy with the increase of the number of QD planes stacked is observed. This redshift has been related to an increase of the QD size during the stacking. It leads to a reduced modal gain for a given wavelength bandwidth detrimental for the laser operation. Similar evolution has been observed during InAs/GaAs (001) or InAs/InP (001) nanostructure stacking. Large improvements have been achieved by using DC method for each plane and by increasing the spacer thickness from 10 to 40 nm (See figure 11) Due to the DC technique and the lower mean strain accumulated the PL energy shift is drastically reduced. Moreover we observe on the AFM image, a two dimensional QD organisation along the direction of easy deformation of the zinc blende lattice.

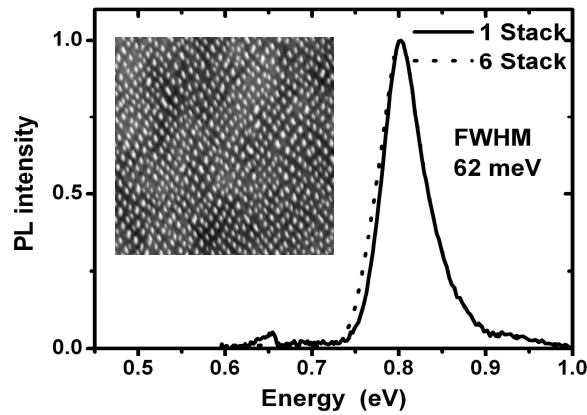


Figure 11. Room temperature PL spectra of InAs/InGaAsP QD, for one QD layer (continuous line) and six QD stacked layers (dashed line). In Inset AFM image recorded on the uncapped 6th planes

Room temperature laser emission has been obtained from those optimized quantum dots.³⁰ For long cavity laser (3.06 mm), a threshold current density of 190A/cm² has been determined (figure 12). From the measurement of the threshold current density as a function of the inverse cavity length, a transparency current density (J_{∞}) for infinite cavity of 21 A/cm² has been deduced. It corresponds to a J_{∞} of 7 A/cm² per QD plane which compare favourably with results reported for QDhs (45 A/cm²) or QWs (60 A/cm²) laser. The temperature dependence of the threshold current density is reported on fig 12. When the temperature raises from 100 to 160 K The J_{th} remains constant as one can be expected for an ideal QD laser. At temperatures higher than 160 K, the characteristic temperatures decreases and becomes close to 55K at room temperature. This value is comparable with those reported for QW lasers. It has been related to the proximity of QDs confined states to the wetting layer energy continuum.

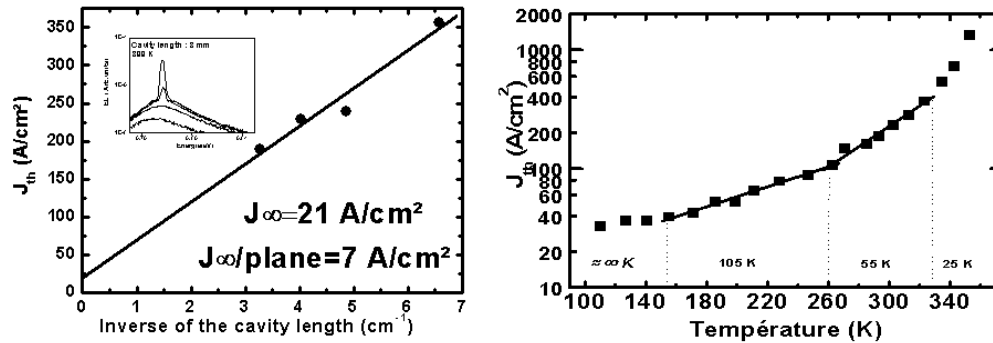


Figure 12. Threshold current density against reciprocal cavity length taken at room temperature for a quantum dot laser grown on (113) substrate (left) and the characteristic temperature versus temperature.

Single mode ridge structures have been elaborated from (113) B substrates. Room temperature laser emission have been achieved at 1.52 μm for cavities as short as 1030 μm . Emission on the QD ground state in CW regime has been observed up to 75 $^{\circ}\text{C}$ with a injected current of 200 mA. The linewidth enhancement factor has been measured for a modulation frequency of 7 GHz. The results are reported on fig 13. A drastic increase in the Henry Factor (HF) is evidenced when the laser is biased above threshold.³¹ A HF of 6.8 at 1522 nm has been determined. The Henry factor does not noticeably change with the bias current as it amounts to 57 to 137 mA. This behaviour has been related to the significant band filling of higher energy levels i.e., the wetting layer that breaks the Gaussian like symmetry of the gain spectrum.

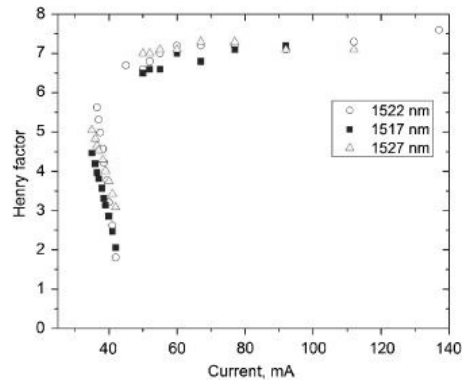


Figure 13. Henry factor below and above threshold of a 1100 μm long InAs/InP (311)B QD FP laser.

4. BEYOND 1.55 μm

Most of works on InAs/InP NS was focused in devices working at 1.55 μm for telecom applications. Attempts to use InAs/InP NS to extend the wavelength further into 1.8-3 μm range, have recently attracted more attention. Lasers emitting in this spectral range are desirable for applications in molecular spectroscopy or remote sensing.³² Room temperature laser emitting around 2 μm has been reported.^{33,34} The threshold current densities are around 500 A/cm² for 1.7 mm long cavity which is comparable to those of laser emitting at 1.55 μm . However the device performances degrade rapidly with the emission wavelength increase and the maximum wavelength reported is 2.05 μm .³⁵ This trend can be related to the gradual shape evolution from high density wires to low density of large QDs with the NS volume.

A way to extend the emission wavelength is based on the incorporation of Sb within InAs QDs. Theoretical calculations showed that the emission wavelength can be extended into the 2-3 μm range due to the low band gap of antimonide compounds.³⁶ Moreover the incorporation of Sb leads to an increase of the lattice mismatch which is favourable for QD formation on InP. However experiments show that the presence of Sb on surface during the InAs QD formation causes dramatic changes in SK process.³⁷ First, when a Sb flux is supplied on surface during InAs NS formation, PL emission does not shift to longer wavelength.³⁸ Thus, the incorporation of Sb within QDs is not yet demonstrated. In addition, when Sb atoms are present on surface, the InAs NS shape changes to more elongated flat quantum wires emitting around 1.8 μm . In extreme case, the Sb atoms lead to a complete suppression of SK transition. In order to illustrate such phenomenon, on figure 14, a high resolution transmission electron microscopy (TEM) image recorded on sample on which 14 ML of InAs has been deposited in presence of a Sb flux is shown. TEM analysis reveals that despite the large amount of InAs deposited, SK transition does not occur and QDs are not formed. Moreover careful analysis of the strain shows that the Sb content is lower than 5 %. This is mainly induced by the surfactant effect of Sb atoms³⁹ and by the large lattice mismatch between InAsSb and InP which make difficult the achievement of InAsSb quantum dots. Therefore further work is needed to InAsSb QD lasers operating in the 2–3 μm region.

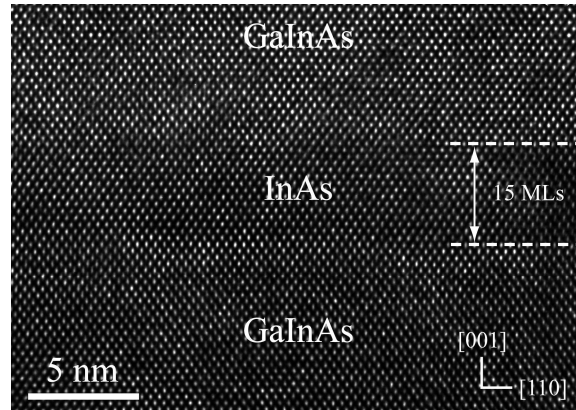


Figure 14. High resolution transmission electron micrograph recorded after the deposition of 15 ML of InAs on InGaAs alloy layer lattice matched on InP in presence of a Sb flux. Without Sb the critical thickness for island formation is lower than 4 ML.

As demonstrated for 1.3 μm QD laser on GaAs substrate, the NS capping is a key step to increase the emission wavelength. Strain reducing or GaAsSb alloy layers have been proposed in InAs/GaAs system.⁴⁰⁻⁴² In fig 15 are reported X-STM images recorded for InAs NS grown on InP (113)B substrates and capped with InP or GaAsSb materials. When InP cap is used, the average height estimated from 20 individual QDs is 2.6 nm. The homogeneity of the contrast reveals that QDs consist in almost pure InAs except at the corners where InAsP alloy is formed. The height of uncapped InAs QDs deduced by AFM is 3.3 nm. Thus, the capping layer growth induced a large reduction of the height and thus a blue shift of the PL emission. It is related to the As/P exchange occurring during InP capping layer growth. At the opposite when QDs are capped with GaAsSb layer, lattice matched with InP, the QDs are taller than those capped with a InP layer. An average height of 3.3 nm and a base diameter are deduced. PL spectra from samples capped with InP and GaAsSb layers are reported fig 15. A large redshift from 0.87 to 0.68 eV is observed when a GaAsSb cap layer is used. The shift is attributed to the preservation of QDs shape and to the type-II band lineup occurring at the InAs/GaAsSb interface. The radiative recombination occurs between electrons confined in the QDs and the holes in the GaAsSb layer. It is confirmed by the dependence of the emission energy with the cubic root of the excitation power reported on fig. 15 insert. These QD were inserted in InP matrix and thus emit at high energy. Next works will consist in integrated GaAsSb capped QD in InGaAs matrix in order to achieve long wavelength laser structures.

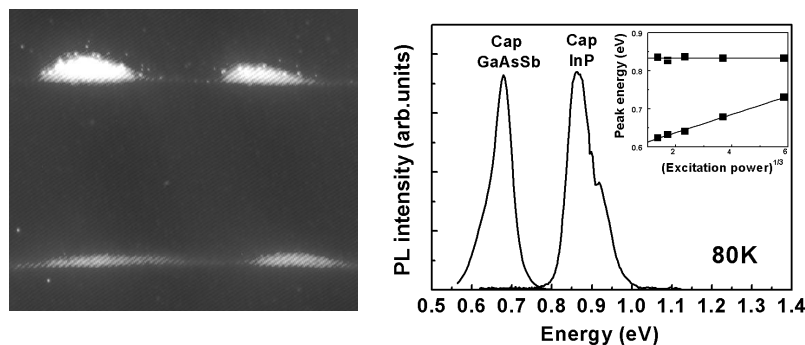


Figure 15. Left : X-STM image of InAs quantum dots formed on InP (311)B. The first QD layer was cap with InP layer and the second with a 1 nm GaAsSb layer. The bright spots correspond to Sb atoms. Right: Photoluminescence spectra recorded at 80K from InAs/InP QDs and from InAs QDs capped with a 2 nm thick GaAsSb layer.

5. CONCLUSION

Due to the low lattice mismatch existing in the InAs/InP system, we have shown that the formation of nanostructure is more complex than in the InAs/GaAs material system. High densities of elongated structures or low densities of large dots are commonly observed on nominal (001) InP substrates. The quantum wires/dashes are in high density and present a modal gain well enough to achieve room temperature laser. State of art, Qwire lasers have been demonstrated achieved. Threshold current density for infinite cavities of 225 A/cm^2 is measured. Although quantum wires are the most easily nanostructures to achieve in high density, QDs can be obtained by using non standard substrates. First, nanostructure formation on miscut substrates has been investigated. We observe that dot formation is favoured when step edges run perpendicular to the direction of the dashes, but no change occurs when the step edges are parallel to the step structures. Secondly, we show that on (113)B substrates, InAs QDs in density and size comparable with those obtained on GaAs substrate can be achieved. The QD lasers grown on (113)B substrates show a reduced threshold current density in comparison with the QW counterpart. Moreover an infinite characteristic temperature is measured at cryogenic temperature. However the characteristic temperature above room temperature and the Henry factors do not present the large improvements predicted for ideal quantum dots. Finally, the first attempts to realize QD lasers on InP substrates emitting at wavelength below $2 \mu\text{m}$ are presented. The surfactant effect of the Sb complicates the achievements of InAsSb quantum dots. A more reliable way to extend the emission wavelength is the use of GaAsSb alloy lattice matched as the InAs QDs capping layers.

REFERENCES

- [1] Mowbray, D. J. and Skolnick, M. S., "New physics and devices based on self-assembled semiconductor quantum dots," J. Phys. D: Appl. Phys. 38, 2059-2076 (2005).
 - [2] Asada, M., Miyamoto, Y. and Suematsu, Y., "Gain and the threshold of three dimensional quantum-box lasers," IEEE J. Quantum Electron. 22, 1915-17 (1986).
 - [3] Kirstaedter, N., Ledentsov, N., N., Grundmann, M., Bimberg, D., Ustinov, V.M., Ruvimov, S.S., Maximov, M.V., Kop'ev, P.S., Alferov, Zh.I., Richter, U., Werner, P., Gosele, U. and Heydenreich., "Low threshold, large T0 injection laser emission from (In,Ga)As quantum dots," Electron. Lett. 30, 1416 (1994).
 - [4] Bimberg, D *et al*, [Quantum Dot Heterostructures] Chichester: Wiley, (1998).
 - [5] Akiyama, T., Ekawa, M., Sugawara, M., Kawaguchi, K., Sudo, H., Kuramata, A., Ebe, H., Arakawa, Y., "An ultrawide-band semiconductor optical amplifier having an extremely high penalty-free output power of 23 dBm achieved with quantum dots," IEEE Photonics Technology Letters, 17, 1614 - 1616 (2005).
 - [6] Shi, L., W., Chen, Y., H., Xu, B., Wang Z. C., Jiao Y. H. and Wang Z. G. "Status and trends of short pulse generation using mode-locked lasers based on advanced quantum-dot active media," J. Phys. D: Appl. Phys. 40, R307 (2007).
 - [7] Alizon, R., Parillaud, O., Gerschütz, F., Kaiser, W., Reithmaier, J. P., Somers, A., Deubert, S., Forchel, A., Krakowski M., and Hadass D., "Semiconductor quantum dots devices: Recent advances and application prospects" physica status solidi (b) 243, 3981 (2006).
 - [8] Kawaguchi, K., Yasuoka, N., Ekawa, M., Ebe, H., Akiyama, T., Sugawara, M., and Arakawa, Y., "Optical properties of columnar InAs quantum dots on InP for semiconductor optical amplifiers," Appl. Phys. Lett. 93, 121908 (2008).
- Akiyama, T. Ekawa, M. Sugawara, M. Kawaguchi, K. Sudo, H. Kuramata, A. Ebe, H. and Arakawa," An ultrawide-band semiconductor optical amplifier having an extremely high penalty-free output power of 23 dBm achieved with quantum dots," Y.IEEE Photonics Technol. Lett. 17, 1614 (2005).

- [9] Ramdane, A., Martinez, A., Azouigui, S., Cong, D.-Y., Merghem, K., Akrou, A., Gosset, C., Moreau, G., Lelarge, F., Dagens, B., Provost, J.-G., Accard, A., Le Gouezigou, O., Krestnikov, I., Kovsh, A., and Fischer, "Recent advances in long wavelength quantum dot based lasers," *M. Proc. SPIE* 6900, 690008 (2008).
- [10] Stintz, A., Rotter, T. J., Malloy, K. J., "Formation of quantum wires and quantum dots on buffer layers grown on InP substrates," *J of Cryst Growth*, 255, 266-272 (2003).
- [11] The samples have been grown by gas source MBE. In such system the Arsine flux is produced from the thermal decomposition of Arsine in a cracker. The arsenic flux is proportional to the arsine flow, measured in Standard Cubic Centimeter Mass
- [12] Krzyzewski, T. J. and Jones, T. S., "Nanostructure formation in InAs/InP(001) heteroepitaxy: Importance of surface reconstruction," *Phys. Rev. B* 78, 155307 (2008).
- [13] Zhang, Z. H., Pickrell, G. W., Chang, K. L., Lin, H. C., Hsieh, K. C. and Cheng, K. Y., "Surface morphology control of InAs nanostructures grown on InGaAs/InP," *Appl. Phys. Lett.* 82, 4555 (2003).
- [14] Gendry, M., Monat, C., Brault, J., Regreny, P., Hollinger, G., Salem, B., Guillot, G., Benyattou, T., Bru-chevallier, C., Bremond, G. and Marty O., "From large to low height dispersion for self-organized InAs quantum sticks emitting at 1.55 μm on InP (001) ," *J. Appl. Phys.* 95, 4761 (2004).
- [15] Grosse, F. and Gyure, M. F., "Island and step morphology in InAs(001) Homoepitaxy," *Phys. Stat. sol* 234, 338-345 (2002).
- [16] Lelarge, F. Dagens, B. Renaudier, J. Brenot, R. Accard, A. van Dijk, A. F. Make, D. Le Gouezigou, O. Provost, J. G. Poinot F., Landreau, J. Drisse, O. Derouin, E. Rousseau, B. and Pommereau F., "Recent Advances on InAs/InP Quantum Dash Based Semiconductor Lasers and Optical Amplifiers Operating at 1.55 μm ," *IEEE J. Sel. Top. Quantum Electron.* 13, 111 (2007).
- [17] Reithmaier, J. P., Somers, A., Deubert, S., Schwertberger, R., Kaiser, W., Forchel, A., Calligaro, M., Resneau, P., Parillaud, O., Bansropun, S., Krakowski, M., Alizon, R., Hadass, D., Bilenca, A., Dery, H., Mikhelashvili, V., Eisenstein, G., Gioannini, M., Montrosset, I., Berg, T. W., van der Poel, M., Mork, J., and Tromborg, B., "InP based lasers and optical amplifiers with wire-/dot-like activeRegions," *J. Phys. D: Appl. Phys.* 38, 2088-2102 (2005).
- [18] Merghem, K., Akrou, A., Martinez, A., Aubin, G., Ramdane, A., Lelarge, F. and Duan, G.-H., "Pulse generation at 346 GHz using a passively mode locked quantum-dash-based laser at 1.55 μm ," *Appl. Phys. Lett.* 94, 021107 (2009).
- [19] Lamy, J. M., Paranthoen, C., Levallois, C., Nakkar, A., Folliot, H., Gauthier, J. P., Dehaese, O., Le Corre, A., and Loualiche, S., "Polarization control of 1.6 μm vertical-cavity surface-emitting lasers using InAs quantum dashes on InP(001)," *Appl. Phys. Lett.* 95, 011117 (2009).
- [20] Salem, B., Olivares, J., Guillot, G., Bremond, G., Brault, J., Monat, C., Gendry, M., Hollinger, G., Hassen, F., and Maaref, H., "Optical properties of self-assembled InAs quantum islands grown on InP(001) vicinal substrates," *Appl. Phys. Lett.* 79, 4435 (2001).
- [21] Cotta, M. A., Mendonca, C. A. C., Meneses, E. A., de Carvalho, M. M. G., "On the onset of InAs islanding on InP: influence of surface steps," *Surface Science*, 388, 84-91 (1997).
- [22] Bierwagen, O. and Masselink, W. T., " Self -organized growth of InAs quantum wires and dots on InP(001): The role of vicinal substrates," *Appl. Phys. Lett.* 86, 113110 (2005).

- [23] Elias, G., Létoublon, A., Piron, R., Alghoraibi, I., Nakkar, A., Chevalier, N., Tavernier, K., Le Corre, A., Bertru, N., and Loualiche, S., "Achievement of High Density InAs/GaInAsP Quantum Dots on Misoriented InP(001) Substrates Emitting at 1.55 μm ," *Jpn. J. Appl. Phys.* 48, 070204 (2009).
- [24] Frechengues, S., Bertru, N., Drouot, V., Lambert, B., Robinet, S., Loualiche, S., Lacombe, D. and Ponchet, A., "Wavelength tuning of InAs quantum dots grown on (311)B InP," *Appl. Phys. Lett.* 74, 3356 (1999).
- [25] Caroff, P., Platz, C., Dehaese, O., Paranthoen, C., Bertru, N., Le Corre, A., Loualiche, S., "Molecular beam epitaxy growth of quantum dot lasers emitting around 1.5 μm on InP(3 1 1)B substrates," *J. Crystal. Growth.* 278, 329-334(2005).
- [26] Caroff, P., Bertru, N., Le Corre, A., Dehaese, O., Rohel, T., Alghoraibi, I., Folliot, H., and Loualiche S., "Achievement of High Density InAs Quantum Dots on InP (311)B Substrate Emitting at 1.55 μm ," *Jpn. J. Appl. Phys.*, Part 2 44, L1069 (2005).
- [27] Nishi, K., Saito, H., Sugou, S. and Lee, J-S., "A narrow photoluminescence linewidth of 21 meV at 1.35 μm from strain-reduced InAs quantum dots covered by In_{0.2}Ga_{0.8}As grown on GaAs substrates," *Appl. Phys. Lett.* 74, 1111 (1999).
- [28] Paranthoen, C., Bertru, N., Dehaese, O., Le Corre, A., Loualiche, S., Lambert, B. and Patriarche, G., "Height dispersion control of InAs/InP quantum dots emitting at 1.55 μm ," *Appl. Phys. Lett.* 78, 1751 (2001).
- [29] Ulloa, J. M., Koenraad, P. M., Gapihan, E., Letoublon, A. and Bertru, N., "Double capping of molecular beam epitaxy grown InAs/InP quantum dots studied by cross-sectional scanning tunneling microscopy," *Appl. Phys. Lett.* 91, 073106 (2007).
- [30] Caroff, P., Paranthoen, C., Platz, C., Dehaese, O., Folliot, H., Bertru, N., Labbe, C., Piron, R., Homeyer, E., Le Corre, A. and Loualiche, S., "High-gain and low-threshold InAs quantum-dot lasers on InP," *Appl. Phys. Lett.* 87, 243107 (2005).
- [31] Martinez, A., Merghem, K., Bouchoule, S., Moreau, G., Ramdane, A., Provost, J.-G., Alexandre, F., Grillot, F., Dehaese O., Piron, R. and Loualiche, S., "Dynamic properties of InAs/InP (311)B quantum dot Fabry--Perot lasers emitting at 1.52 μm ," *Appl. Phys. Lett.* 93, 021101 (2008).
- [32] Lei, W. and Jagadish, C., "Lasers and photodetectors for mid-infrared 2-3 μm applications," *J. Appl. Phys.* 104, 091101 (2008).
- [33] Reithmaier, J.P., Kaiser, W., Hein, S., Somers, A., Höfling, S. and Forchel, A., "Singlemode InAs/InP quantum dash distributed feedback lasers emitting in 1.9 μm range," *Electronics Letters* 44, 527 (2008).
- [34] Rotter, T. J, Stintz, A. and Malloy, K. J., "InP based quantum dash lasers with 2 μm wavelength," *IEE Proc.- Optoelectron.* 150, 318-21 (2003).
- [35] Koeth, J., Somers, A., Zeller, W., Legge, M., Kaiser, W. and Forchel A., "Singlemode emission at 2 μm wavelength with InP based quantum dash DFB lasers," *Electronics Letters* 44, 354 (2008).
- [36] Cornet, C., Dore, F., Ballestar, A., Even, J., Bertru, N., Le Corre, A. and Loualiche, S., "InAsSb/InP quantum dots for midwave infrared emitters: A theoretical study," *J. Appl. Phys.* 98, 126105 (2005).
- [37] Kawaguchi, K., Ekawa, M., Akiyama, T., Kuwatsuka, H., Sugawara, M., "Controlling shape of InAs_{1-x}Sb_x quantum structures on InP for quantum dots with 1.55 μm emission," *J. Cryst. Growth* 298, 558-561 (2007).
Kawaguchi, K., Ekawa, M., Akiyama, T., Kuwatsuka, H., Sugawara, M., "Surfactant-related growth of InAs_{1-x}Sb_x quantum structures on InP(001) by metalorganic vapor-phase epitaxy," *J. Cryst. Growth* 291, 154-159 (2006).

- [38] Lei, W., Tan, H. H. and Jagadish, C., "Formation and shape control of InAsSb/InP (001) nanostructures," *Appl. Phys. Lett.* 95, 013108 (2009).
- [39] Harmand, J. C., Li, L. H., Patriarche, G. and Travers, L., "GaInAs/GaAs quantum-well growth assisted by Sb surfactant: Toward 1.3 μm emission," *Appl. Phys. Lett.* 84, 3981 (2004).
- [40] Nishi, K., Saito, H., Sugou, S. and Lee, J-S., "A narrow photoluminescence linewidth of 21 meV at 1.35 μm from strain-reduced InAs quantum dots covered by In_{0.2}Ga_{0.8}As grown on GaAs substrates," *Appl. Phys. Lett.* 74, 1111 (1999).
- [41] Liu, H. Y., Steer, M. J., Badcock, T. J., Mowbray, D. J., Skolnick, M. S., Suarez, F., Ng, J. S., Hopkinson, M. and David, J. P. R., "Room-temperature 1.6 μm light emission from InAs/GaAs quantum dots with a thin GaAsSb cap layer," *J. Appl. Phys.* 99, 046104 (2006).
- [42] Ulloa, J. M., Celebi, C., Koenraad, P. M., Simon, A., Gapihan, E., Letoublon, A., Bertru, N., Drouzas, I., Mowbray, D. J., Steer, M. J. and Hopkinson, M., "Atomic scale study of the impact of the strain and composition of the capping layer on the formation of InAs quantum dots," *J. Appl. Phys.* 101, 081707 (2007).